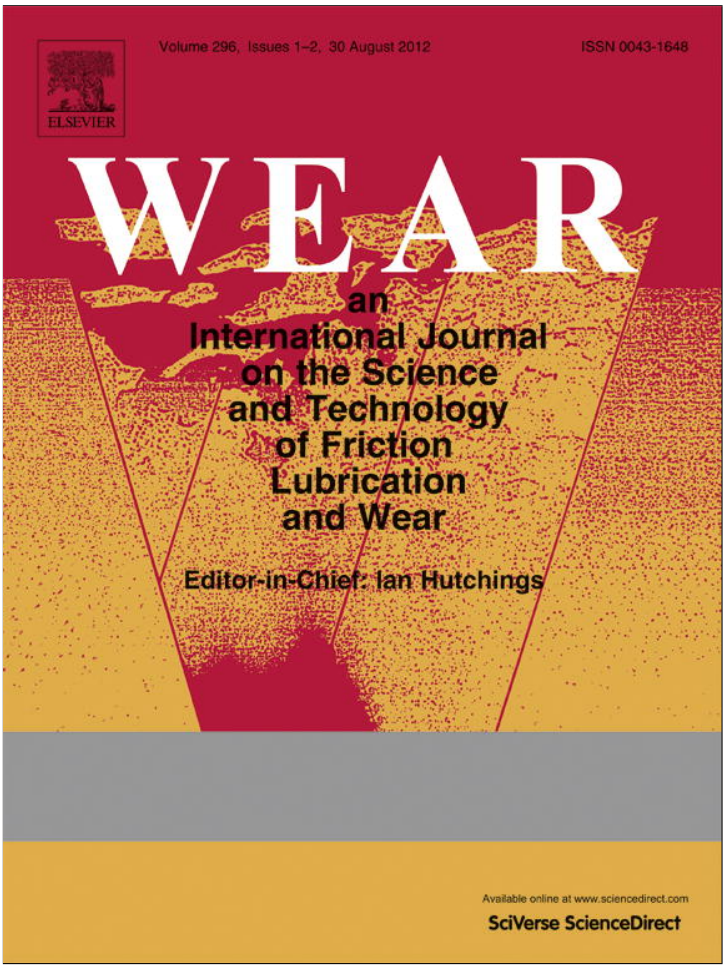

Wear 296 (2012) 575–582

Contents lists available at SciVerse ScienceDirect

Wear

journal homepage: www.elsevier.com/locate/wear

Tribological performance of silicone composite coatings filled with wax-containing microcapsules

N.W. Khun, H. Zhang, J.L. Yang, E. Liu *

School of Mechanical and Aerospace Engineering, Nanyang Technological University, 50 Nanyang Avenue, Singapore 639798, Singapore

ARTICLE INFO

Article history:
Received 21 December 2011
Received in revised form
5 July 2012
Accepted 25 July 2012
Available online 2 August 2012

Keywords:
Silicone matrix composite
Surface topography
Sliding wear
Wear testing

ABSTRACT

The effect of wax-containing microcapsules incorporated in silicone composite coatings deposited on aluminum (Al) alloy substrates on the tribological performance of the coatings was systematically investigated. The wax-containing microcapsules were prepared via in situ polymerization. The tribological behavior of the composite coatings was evaluated using ball-on-disk tribological test. It was found that the increase in microcapsule concentration in the composite coatings apparently reduced the friction coefficient of the coatings because the lubricant released from the broken microcapsules during the tribological test of the coatings lubricated the rubbing surfaces. The results showed that the silicone composite coatings rubbed by a smaller Cr6 steel ball (3 mm diameter) under a lower normal load (100 mN) produced higher friction coefficients via reduced complication of their underlying strong substrates compared to the same coatings tested against a larger Cr6 steel ball (6 mm diameter) under a higher normal load (1 N).

1. Introduction

Nowadays, components made of rubber-like materials are increasingly replacing metallic components due to their ease of manufacturing, lightweight and low cost in addition to their traditional roles as seals, diaphragms, etc [1–3]. Silicone elastomers, which have high electrical, corrosion and heat resistances and rubber-like properties, have been commonly used to manufacture implants, sealants, gaskets and top coatings in applications where tribological performance is of special advantage. However, elastomers usually have a high dry sliding friction, which requires the use of lubrication in various applications [4,5].

It is important to note that external lubrication on rubbing surfaces may limit the application of materials due to degradation caused by absorption and osmosis of the lubricants into the rubbing materials [5,6]. Guo and co-workers [1] reported that incorporation of microcapsules containing a liquid lubricant into epoxy composites reduced the friction of the composites because the pre-embedded microcapsules were broken during repeated sliding and the lubricant encapsulated was released to the rubbing surfaces. Therefore, it is expected that the tribological performance of elastomers could be improved by the incorporation of microcapsules containing a liquid lubricant. The fundamental understanding of a synergy between incorporation of lubricant-containing microcapsules in elastomer composites and their self-lubricating performance is essential for successful applications. However, the study of the tribological performance of elastomer matrix composites filled with microcapsules has not been reported.

In this study, microcapsules containing a liquid wax lubricant with varying concentrations were embedded in silicone matrices to form a new type of composite material. The silicone and composites were coated on aluminum (Al) alloy substrates and the effect of microcapsule incorporation on the tribological performance of the coatings was systematically investigated. The surface activity and morphology of the coated samples were also studied.

2. Experimental details

2.1. Sample preparation

Microcapsules were prepared by in situ polymerization in an oil-in-water emulsion system. All chemicals and reagents were purchased from Sigma Aldrich and used as received. First, 200 mL of de-ionized (DI) water and 50 mL of an aqueous solution containing 2.5 wt% ethylene maleic anhydride copolymer (EMA) were mixed in a beaker that was stirred at 1000 rpm for a few minutes. After that, 5 g of urea ($CO(NH_2)_2$), 0.5 g of ammonium chloride (NH_4Cl) and 0.5 g of resorcinol ($C_6H_6O_2$) were dissolved in the solution under agitation. The pH of the mixture was adjusted from about 2.6 to 3.5 by dropping 1 M sodium hydroxide (NaOH). One or two drops of 1-octanol ($CH_3(CH_2)_7OH$) were added into the mixture to eliminate

* Corresponding author. Tel.: +65 67905504; fax: +65 67924062.
E-mail address: MEJLiu@ntu.edu.sg (E. Liu).

0043-1648/$ - see front matter © 2012 Elsevier B.V. All rights reserved.
http://dx.doi.org/10.1016/j.wear.2012.07.029

surface bubbles. A slow stream of wax (Episol B2531) of 60 mL used for core materials was added into the mixture and allowed to disperse for about 10 min. Then, 12.67 g of an aqueous solution containing 37 wt% formaldehyde (CH_2O, PUF) used for shell-forming materials was slowly added into the mixture. The final mixture was heated to the target temperature of 55 °C at a heating rate of 35 °C/h using a hotplate and continuously agitated for 4 h, followed by a natural cooling. Once the temperature reached ambient temperature (~22 °C), the microcapsules were separated under vacuum with a coarse-fritted filter, which were then rinsed with DI water and dried for 24 h.

A silicone elastomer (Sylgard 184, Dow Corning), whose two components were mixed with a weight ratio of 10:1 in atmospheric environment, was used as the matrix material in this study. Both silicone and silicone matrix composites containing 10 and 20 wt% microcapsules were dip-coated on aluminum alloy (AA5083) substrates having a square top surface of 3 cm × 3 cm and the coated samples were designated as Sil, SilCap10 and SilCap20, respectively. The thickness of the coatings was about 0.9–1 mm. Prior to the coatings, the surfaces of the Al alloy substrates were polished using alumina particles of about 0.03 μm in diameter (Buehler Alpha Micropolish II) at the final polishing stage.

2.2. Characterization

The surface roughness of the samples was measured using surface profilometry (Talyscan 150) with a diamond stylus of 4 μm in diameter at a scan size of 1 mm × 1 mm. Five measurements on each sample were conducted to get an average root-mean-square (R_q) value.

The surface morphology of the samples was studied using white light confocal imaging profilometry (Nikon L150) and scanning electron microscopy (SEM) (JEOL-JSM-5600LV).

The water contact angle of the samples was measured with sessile liquid drop test (FTA 200).

The tribological performance of the samples slid against a steel ball (Cr6) of 6 mm in diameter for about 38 m in sliding distance under a normal load of 1 N was investigated using a ball-on-disk microtribometer (CETR UMT3) at room temperature (RT, ~22 °C). In addition, the same samples were tested against a smaller steel ball (Cr6) of 3 mm in diameter for about 12 m in sliding distance under a lower normal load of 100 mN. The sliding circular path and velocity used for all the tribological tests were 2 mm in radius and 2 cm/s, respectively.

3. Results and discussion

The wax-containing microcapsules used in this study have diameters ranging from about 30 to 250 μm as shown in the SEM micrograph in Fig. 1.

The R_q value of the silicone coated sample is about 0.3 μm that is larger than that (~0.14 μm) of the uncoated Al alloy substrate as depicted in Fig. 2, indicating that the surface morphology of the underlying substrate has no significant influence on the surface roughness of the silicone coating. The R_q values of the composite coatings significantly increase from about 11.29 to 19.08 μm with increased microcapsule concentrations from 10 to 20 wt% due to more protruded microcapsules from the coating surface.

Fig. 3 shows the surface topographies of the uncoated Al alloy substrate and the silicone and silicone composite coated samples, where the large asperities on the surfaces of the composite coated samples are attributed to the microcapsules protruded above the surfaces.

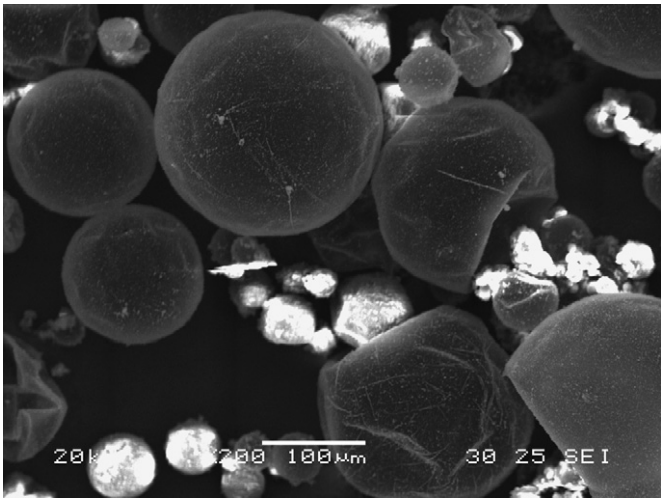

Fig. 1. SEM micrograph of wax-containing microcapsules.

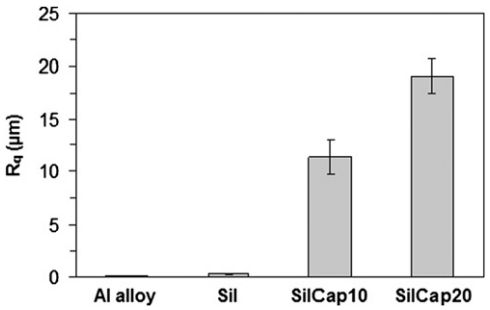

Fig. 2. R_q of uncoated Al alloy substrate, and silicone and silicone composite coated samples.

The water contact angles of the uncoated Al alloy substrate and the silicone and silicone composite coated samples are shown in Fig. 4. When the Al alloy substrate is coated with the silicone, the water contact angle is increased from about 46.2° to 95.8°, implying that the silicone coating significantly reduces the surface energy or wettability of the Al alloy substrate [7,8]. The composite coatings embedded with microcapsules of 10 and 20 wt% show higher water contact angles of about 96.1° and 102.5°, respectively, probably due to the enhanced non-polarity of the coating surfaces caused by the non-polar wax additive.

It is known that the surface roughness has an influence on the contact angle so that a smoother surface can give rise to a smaller contact angle [9,10]. It can be seen that the higher surface roughnesses of the coated samples than that of the uncoated Al alloy substrate (Figs. 2 and 3) also contribute to the larger water contact angles of the coated samples (Fig. 4). Such a contribution is more significant from the composite coating with 20 wt% microcapsules.

Fig. 5 shows the mean friction coefficients of the uncoated Al alloy substrate and the silicone and silicone composite coated samples containing 10 and 20 wt% microcapsules slid against a steel ball of 6 mm in diameter in a circular path of 2 mm in radius for about 38 m in sliding distance at a sliding velocity of 2 cm/s under a normal load of 1 N. The Al alloy substrate has a mean friction coefficient of about 0.56 as shown in Fig. 5a. The friction coefficient of the silicone coated sample jumps to about 1.37, which is probably attributed to the hysteresis friction that results from the energy loss associated with the deformation process of a certain volume of the silicone coating [11–14]. In addition, the occurrence of adhesion at the contact junctions also contributes to the higher friction coefficient of the silicone coating via the

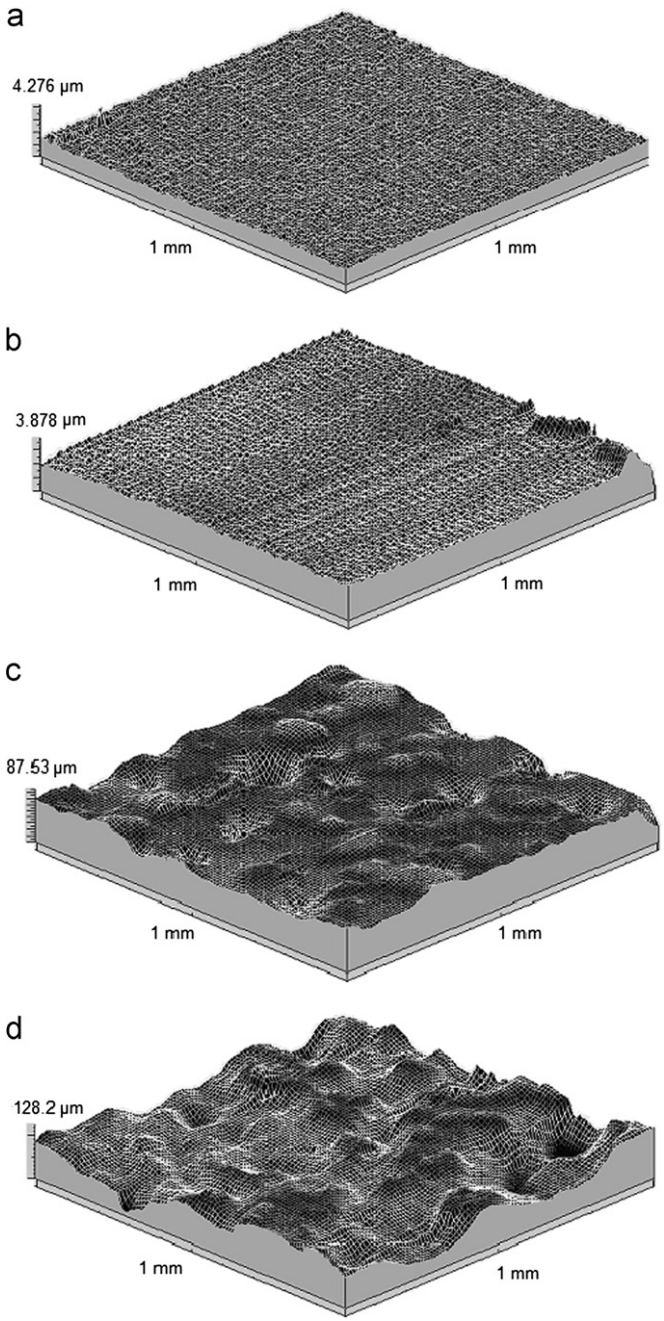

Fig. 3. Surface topographies of (a) uncoated Al alloy substrate, (b) silicone coating and (c) and (d) silicone composite coatings with 10 and 20 wt% microcapsules, respectively.

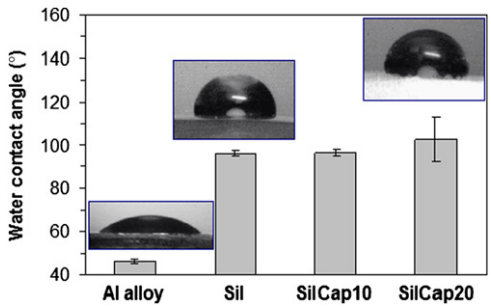

Fig. 4. Water contact angles of uncoated Al alloy substrate, and silicone and silicone composite coated samples. The insets show the water droplets on the sample surfaces.

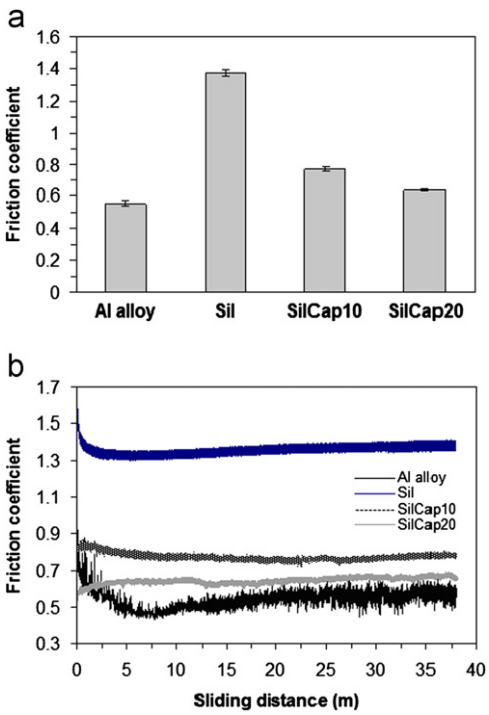

Fig. 5. (a) Mean friction coefficients of uncoated Al alloy substrate and silicone and silicone composite coated samples measured against a 6 mm Cr6 steel ball in a circular path of 2 mm in radius for about 38 m in sliding distance at a sliding velocity of 2 cm/s under a normal load of 1 N, and (b) friction coefficients of the same materials as a function of sliding distance.

effective shear strength of contact interfaces at a macroscopic level [13,15,16]. However, the incorporation of microcapsules in the silicone composite coatings significantly reduces the friction coefficients of the coatings such that the composite coatings with 10 and 20 wt% microcapsules have friction coefficients of about 0.76 and 0.63, respectively, as shown in Fig. 5a. It is clear that the lubricant released from the broken microcapsules during the wear of the coatings lubricates the rubbing surfaces and prevents a direct contact between steel ball and coating, leading to a decrease in the friction of the coatings [1]. Kummer [17] reported that molecular interactions between elastomeric and counter materials during their contact could generate high friction by means of making and breaking of molecular junctions at a molecular level. It has been found in Fig. 4 that the increased contact angles of the coatings result from the enhanced non-polarity of the coating surfaces induced by the increased non-polar wax additive. It is supposed that the possible existence of the non-polar wax additive on the coating surfaces effectively reduces the adhesion component of the total friction at both macroscopic and molecular levels. Therefore, the increased microcapsule concentrations in the composite coatings lower the friction coefficients of the coatings.

It is clear that a contact between the rigid steel ball and flat silicone coating during the sliding leads to a high friction arising from a combination of two friction components: adhesion and hysteresis [11–14]. Therefore, the surface roughnesses of the rubbing bodies play a crucial role in friction during sliding [18]. As seen in Figs. 2 and 3, the surface roughness of the composite coatings significantly increases with increased microcapsule concentration so that the largest asperities are found on the surface of the composite coating with 20 wt% microcapsules. As the large asperities on the surfaces of the composite coatings apparently reduce the real contact areas and possible adhesion at the contact junctions, the developed surface asperities of the composite coating with the higher microcapsule concentration lead to the

decreased friction coefficient of the coating. In addition, the highest surface roughness of the composite coating with 20 wt% microcapsules results in the lowest friction coefficient via the most effective entrapment of the wax lubricant between the surface asperities.

The friction coefficient of the uncoated Al alloy substrate slid against the steel ball significantly decreases in the running-in period and then reaches the steady state as shown in Fig. 5b. At the beginning of the sliding, the contact between the steel ball and Al alloy substrate causes the high friction through mechanical interlocking between the two mating surface asperities [15]. However, the repeated sliding of the steel ball on the Al alloy substrate leads to the smoothening of the two mating surfaces via wear so that the decreased friction coefficient with increased sliding distance is observed in the running-in period as shown in Fig. 5b. The observed slight fluctuation in the friction coefficient of the Al alloy substrate indicates the occurrence of stick-slip phenomenon attributed to the plowing motion of the harder steel ball on the softer Al alloy substrate [19]. For the silicone and composite coated samples, the fluctuations in the friction coefficients appear to be less significant.

Fig. 6a shows the surface morphology of the worn Al alloy substrate after sliding against the 6 mm steel ball for about 38 m in sliding distance, where a significant wear track (wear depth = 16.9 ± 5 μm) is found (the inset in Fig. 6a). The worn surface of the Al alloy substrate is rough with severe plastic flow and abrasive marks as observed in Fig. 6b, resulting from the abrasive wear. In addition, the agglomeration and compaction of wear debris result in the formation of a localized tribo-layer (Fig. 6) [20]. Therefore, the formation and detachment of the tribo-layer may also contribute to the wear of the Al alloy substrate [20].

The abrasive marks are apparently found on the surface of the silicone coated sample slid against a 6 mm steel ball as shown in Fig. 7, but its wear is not measurable. Generally, the sliding of the Cr6 steel ball on the Al alloy substrate apparently generates the abrasive wear of the substrate. When the steel ball is slid on the silicone coated sample, the silicone readily flows to conform to the contour of the steel ball [12]. Such a flowing action of the silicone generates a higher friction via hysteresis, but giving rise to a lower wear by suppressing the abrasive action of the steel ball. However, the sliding of the steel ball on the silicone coated sample under dry condition still causes the tearing of the surface skin of the coating through the abrasive motion of the steel ball

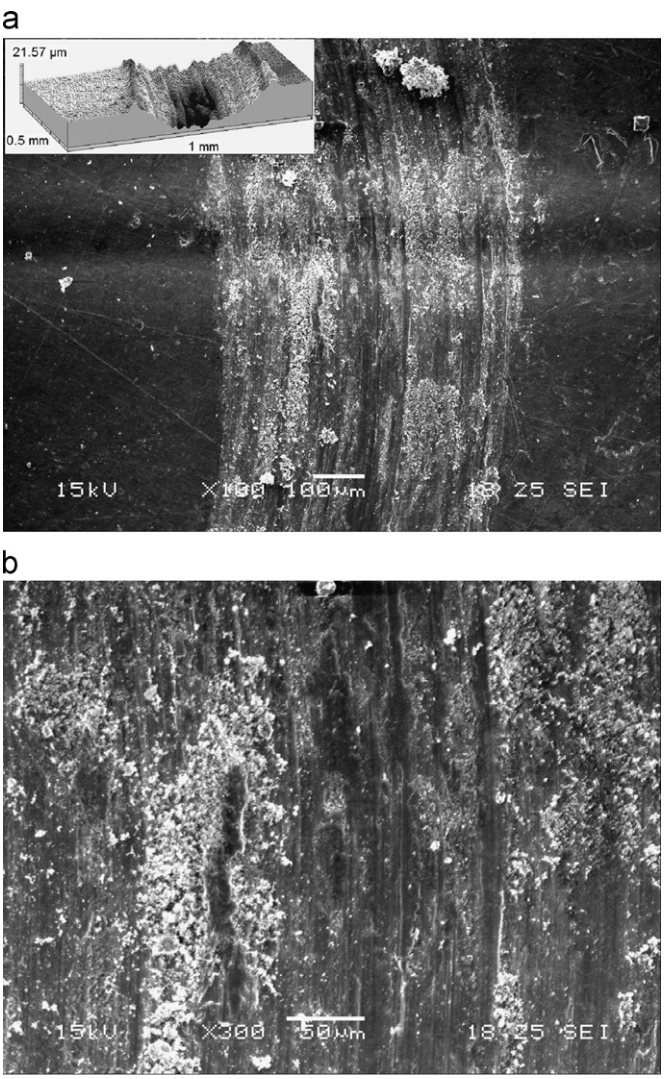

Fig. 6. SEM micrographs showing worn surface morphologies of uncoated Al alloy substrate after rubbing against a steel ball of 6 mm in diameter in a circular path of 2 mm in radius for about 38 m in sliding distance at a sliding velocity of 2 cm/s under a normal load of 1 N at (a) low and (b) higher magnifications. The inset in (a) shows the surface topography of the worn Al alloy substrate.

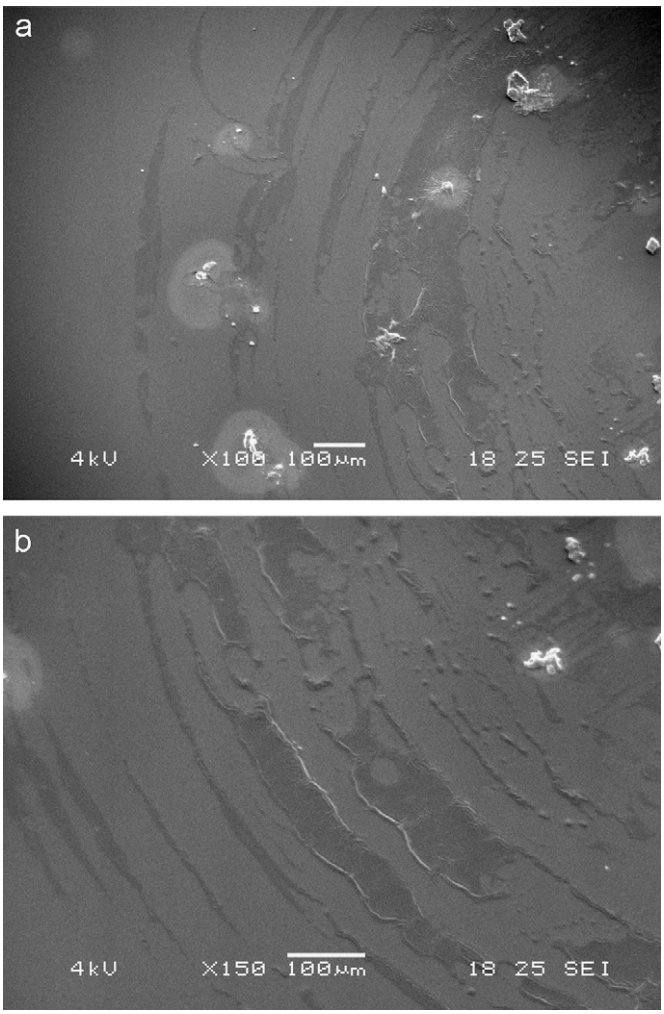

Fig. 7. SEM micrographs showing worn surface morphologies of silicone coated sample after sliding against a 6 mm steel ball in a circular path of 2 mm in radius for about 38 m in sliding distance at a sliding velocity of 2 cm/s under a normal load of 1 N at different locations.

on the coating surface and the interfacial adhesion between the steel ball and coating [21].

Fig. 8 shows the surface morphologies of the worn silicone composite coating embedded with 10 wt% microcapsules after sliding against a 6 mm steel ball for about 38 m in sliding distance.

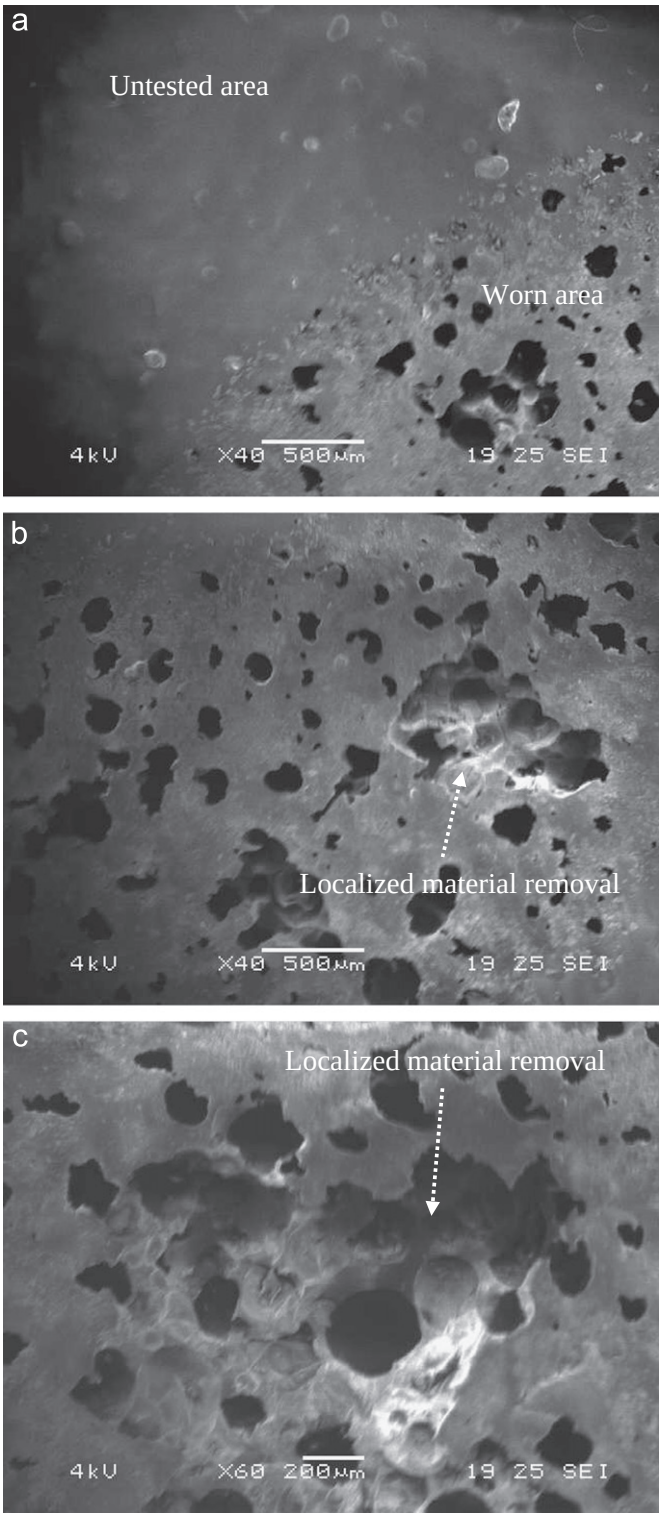

Fig. 8. SEM micrographs showing worn surface morphologies of silicone composite coated sample with 10 wt% microcapsules after sliding against a 6 mm steel ball in a circular path of 2 mm in radius for about 38 m in sliding distance at a sliding velocity of 2 cm/s under a normal load of 1 N at different locations.

In Fig. 8a, the protrusion of the microcapsules above the surface is obviously found on the untested surface area of the composite coating. Since the sizes of the microcapsules used in this study range from about 30 to 250 μm in diameter, a 180 μm ($\pm$20 μm) wear depth of the composite coating is approximately within the size range of the microcapsules. As a result, the worn surface of the composite coating is mainly covered by single holes resulting from the breakage of the microcapsules during the repeated sliding as shown in Fig. 8a and b. However, the localized removal of the materials from deeper regions can also be found in some places of the wear track, as shown in Fig. 8b and c, probably due to the agglomeration of the microcapsules.

Fig. 9a shows the surface morphology of the silicone composite coating embedded with 20 wt% microcapsules, where much more protruded microcapsules above the surface can be observed. The protruded microcapsules lead to easy removal of the coating material during the repeated sliding. Therefore, the composite coating with 20 wt% microcapsules has a largest wear depth of about 280 $\pm$ 41 μm. It can be deduced that the increased surface roughness of the composite coating with increased microcapsule concentration lowers the friction of the coating through the reduced real contact area between the steel ball and coating and the increased entrapment of the wax lubricant on the coating surface. However, more protruded microcapsules also promote the susceptibility of the coating to wear due to the easy breakage of the microcapsules in the coating.

A smaller steel ball of 3 mm in diameter and a lower normal load of 100 mN are used to investigate the influence of deformation volume of the elastomeric coatings on their friction and wear characteristics. A shorter sliding distance of about 12 m is used for the tests with the 3 mm steel ball in order to prevent the contact of the coatings with the ball holder via the progressive wear of the coatings during the prolonged sliding. Nevertheless, a 12 m sliding is sufficient to measure the steady state friction coefficients of the coatings as shown in Fig. 10. In addition, the friction coefficients of the coatings slid against the both 6 and 3 mm steel balls for about 12 m in sliding distance can be properly compared.

Fig. 10a shows the friction coefficients of the silicone and silicone composite coated samples measured against a 3 mm steel ball in a circular path of 2 mm in radius for about 12 m in sliding distance at a sliding velocity of 2 cm/s under a normal load of 100 mN. The friction coefficient of the silicone coated sample is about 1.97, while the composite coated samples with 10 and 20 wt% microcapsules have much lower friction coefficients of about 1.08 and 0.75, respectively. These friction coefficients of the coated samples (Fig. 10a) are consistently higher than those of the same samples (about 1.35, 0.78 and 0.63 for the silicone coated sample and silicone composite coated samples with 10 and 20 wt% microcapsules, respectively) measured against a 6 mm steel ball for a similar sliding distance (about 12 m) under 1 N normal load (Fig. 5a). It is known that the occurrence of hysteresis friction is a consequence of the energy loss associated with the deformation process of an elastomer [12]. When a steel ball is slid on an elastomeric coating coated on a rigid substrate surface under a high normal load, the thickness of the coating can affect its friction coefficient through the variations in the deformation volume of the coating [11,22,23]. It is reported [11–22] that the ratio of the elastomeric coating thickness to the diameter of circular contact area must be at least 10:1 to avoid complication arising due to the supporting boundary condition (e.g. stiffness and compliance of the substrate) underneath the coating. With a smaller ratio, the friction coefficient of the coating under a given load could be underestimated. It is, therefore, supposed that the sliding of the 3 mm steel ball on the coatings under the lower normal load of 100 mN gives rise to higher friction coefficients

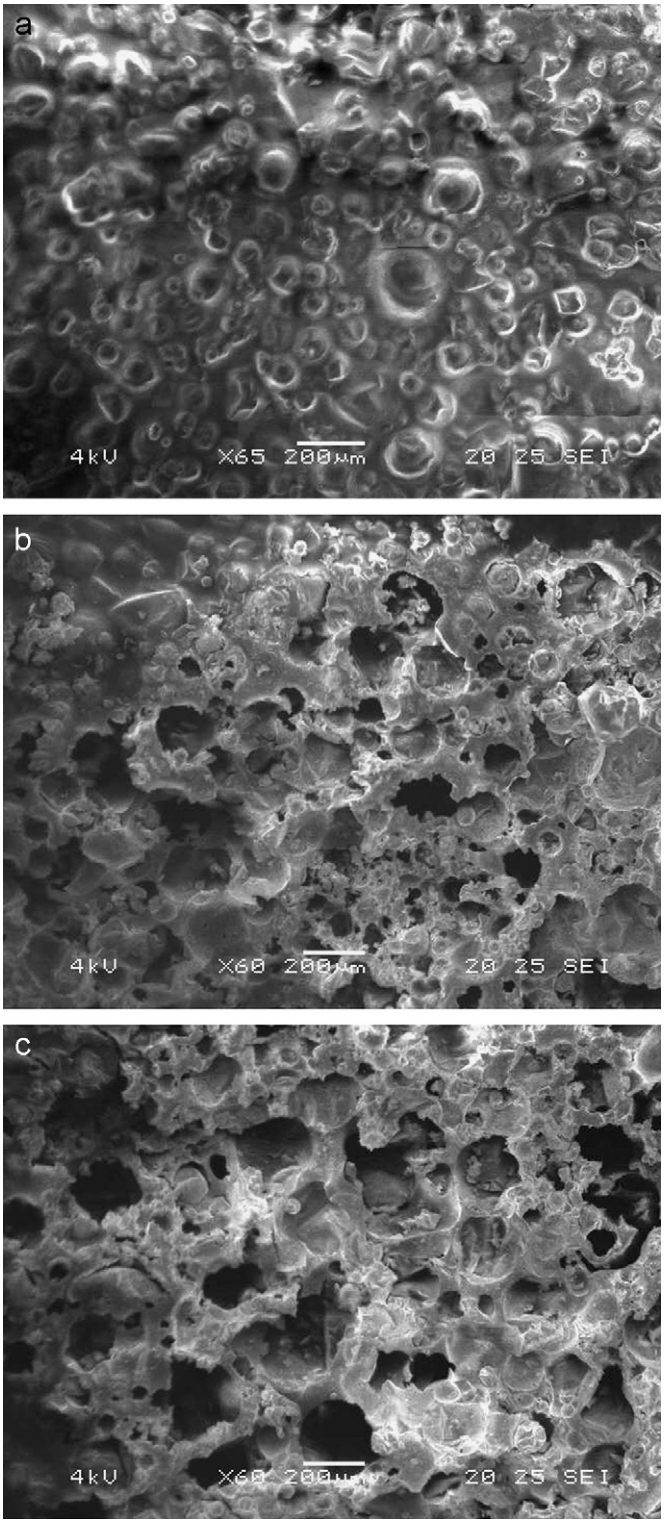

Fig. 9. SEM micrographs showing surface morphologies of silicone composite coated sample with 20 wt% microcapsules (a) before and (b, c) after sliding against a 6 mm steel ball in a circular path of 2 mm in radius for about 38 m in sliding distance at a sliding velocity of 2 cm/s under a normal load of 1 N at different locations.

(Fig. 10a) compared to those of the coatings measured against the 6 mm steel ball under the higher normal load of 1 N (Fig. 5a) because the smaller contact areas between the 3 mm steel ball and the coatings probably enlarge the ratios of the coating thicknesses to the diameters of the circular contact areas.

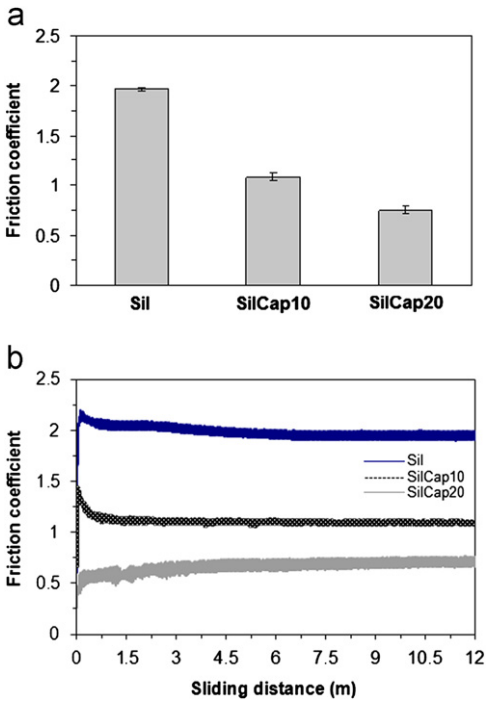

Fig. 10. (a) Mean friction coefficients of silicone and silicone composite coated samples measured against a 3 mm steel ball in a circular path of 2 mm in radius for about 12 m in sliding distance at a sliding velocity of 2 cm/s under a normal load of 100 mN, and (b) friction coefficients of the same samples as a function of sliding distance.

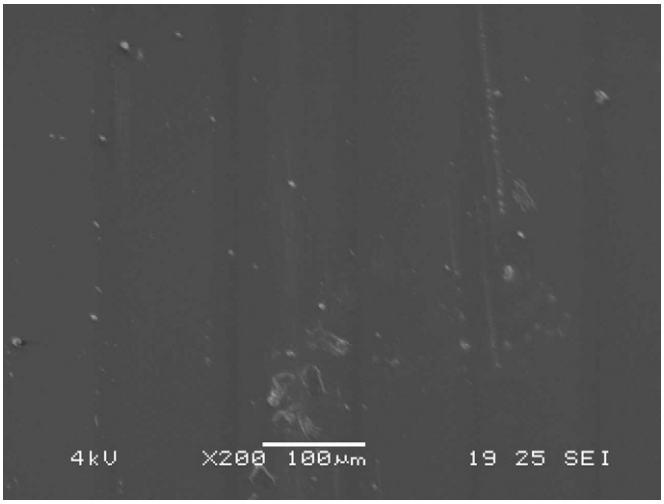

Fig. 11. SEM micrograph showing worn surface morphology of silicone coated sample after sliding against a 3 mm steel ball in a circular path of 2 mm in radius for about 12 m in sliding distance at a sliding velocity of 2 cm/s under a normal load of 100 mN.

The geometric effect of deforming elastomer surface around the ball surface in contact on the frictional behavior of the elastomer should be taken into account since an increase in the wrap angle of the elastomer around the rigid ball can increase the friction coefficient of the elastomer [11]. Therefore, the contact of the 3 mm steel ball with the coatings causes larger wrap angles of the coatings compared to the contact of the 6 mm steel ball with the same coatings.

During dynamic sliding contact, the sliding of a hard steel ball on a soft elastomer can induce a periodic deformation of the elastomer [24–26]. Consequently, the energy loss associated with

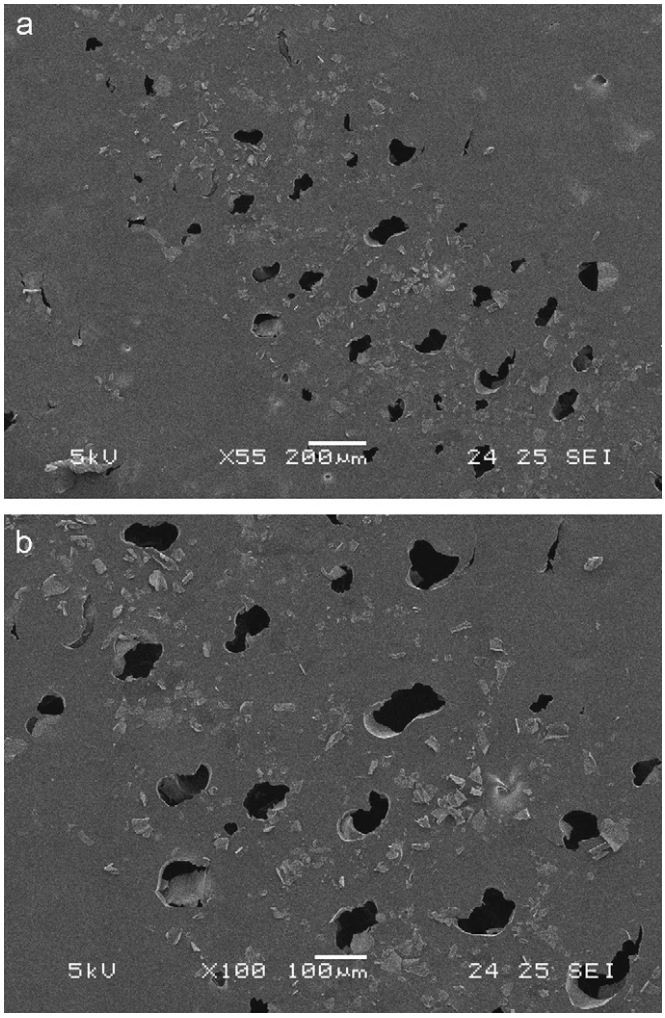

Fig. 12. SEM micrographs showing worn surface morphology of silicone composite coated sample with 10 wt% microcapsules after sliding against a 3 mm steel ball in a circular path of 2 mm in radius for about 12 m in sliding distance at a sliding velocity of 2 cm/s under a normal load of 100 mN at different magnifications.

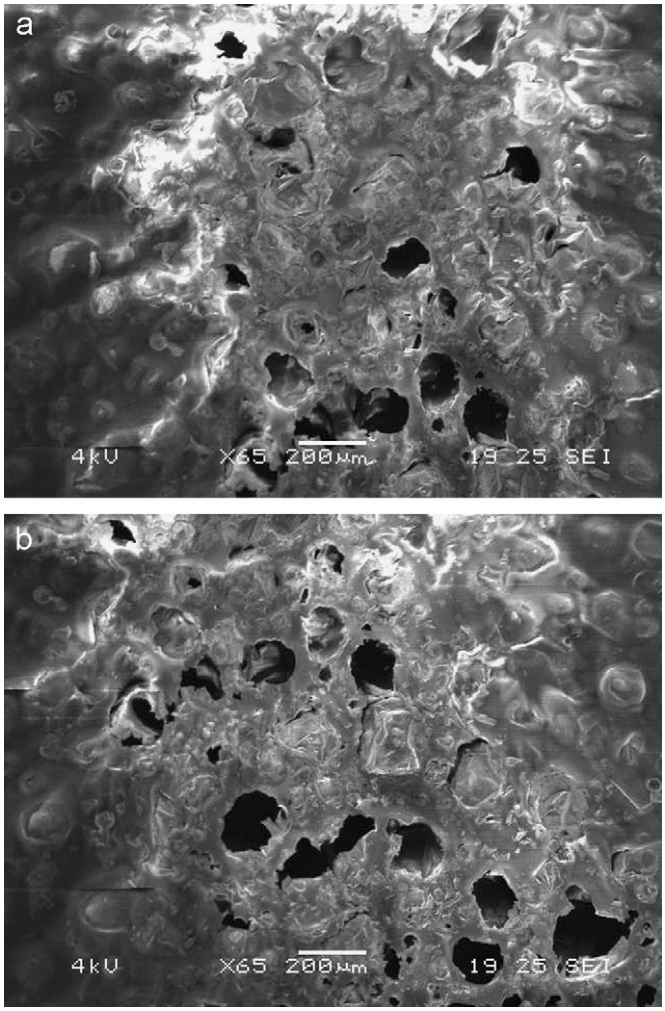

Fig. 13. SEM micrographs showing worn surface morphologies of silicone composite coated sample with 20 wt% microcapsules after sliding against a 3 mm steel ball in a circular path of 2 mm in radius for about 12 m in sliding distance at a sliding velocity of 2 cm/s under a normal load of 100 mN at different locations.

the periodic deformation of the elastomer induces hysteresis friction [26]. It can be seen that the sliding contact of the 3 mm steel ball on the coatings gives rise to a higher hysteresis friction through the deformation of the coatings in a shorter wave form.

Fig. 11 shows the surface morphology of the worn silicone coated sample after sliding against a 3 mm steel ball for about 12 m in sliding distance under the normal load of 100 mN. The abrasive marks observed on the worn sample surface indicate that the abrasive wear can be generated by the rubbing of the steel ball on the coated sample surface under a low normal load.

As seen in Fig. 12, the wear of the silicone composite coated sample embedded with 10 wt% microcapsules is mainly attributed to the breakage of the protruded microcapsules above the coating surface caused by the repeated sliding of the steel ball. With the microcapsule concentration in the composite coatings increased from 10 to 20 wt% the wear depth of the coatings increases from about 90 ($\pm$10) to 130 ($\pm$18)µm, along with the more pronounced breakage of the microcapsules as shown in Fig. 13, which confirms that a higher microcapsule concentration in the composite coatings can lower the wear resistance of the coatings. The experimental results clearly indicate that the tribological behavior of the silicone composite coated samples is effectively influenced by steel ball size and applied normal load.

4. Conclusions

The effect of microcapsule fillers on the tribological performance of silicone composite coatings prepared on Al alloy substrates was systematically investigated. It was found that a higher microcapsule content in the composite coatings apparently promoted the surface roughness of the coated samples due to more protruded microcapsules from the coating surfaces, but, at the same time, lowered the surface activity of the coated surfaces via enhanced non-polarity of the coating surfaces induced by the increased non-polar wax additive. Though the silicone coated sample slid against a Cr6 steel ball showed a relatively high friction coefficient, the increased microcapsule content in the silicone composite coatings significantly reduced the friction coefficient of the coated samples because the wax lubricant released from the broken microcapsules caused by the wear of the coatings lubricated the rubbing surfaces and prevented a direct contact between the steel ball and coating. The composite coatings rubbed by a smaller steel ball (3 mm) under a lower normal load (100 mN) generated higher friction coefficients compared to the same coatings measured against a larger steel ball (6 mm) under a higher normal load (1 N) due to reduced complication arising from the underlying substrates. It was also found that the silicone composite coated samples embedded with

a higher microcapsule content were more susceptible to the abrasive wear induced by a steel ball due to easier breakage of the microcapsules protruded from the coating surfaces.

References

[1] Q.B. Guo, K.T. Lau, B.F. Zheng, M.Z. Rong, M.Q. Zhang, Imparting ultra-low friction and wear rate to epoxy by the incorporation of microencapsulated lubricant, Macromolecular Materials and Engineering 294 (2009) 20–24.

[2] N.H. Sung, N.P. Suh, Effect of fiber orientation on friction and wear of fiber reinforced polymeric composites, Wear 53 (1979) 129–141.

[3] B. Verhedye, M. Rombouts, A. Vanhulsel, D. Havermans, J. Meneve, M. Wangenheim, Influence of surface treatment of elastomer on their frictional behavior in sliding contact, Wear 266 (2009) 468–475.

[4] X.D. Pan, Wet sliding friction of elastomer compounds on a rough surface under varied lubrication conditions, Wear 262 (2007) 707–717.

[5] Z.Z. Zhang, W.M. Liu, Q.J. Xue, Effects of various kinds of fillers on the tribological behavior of polytetrafluoroethylene composites under dry and oil lubricated conditions, Journal of Applied Polymer Science 80 (2001) 1891–1897.

[6] Y.Z. Wan, H.L. Luo, Y.L. Wang, Y. Huang, Q.Y. Li, F.G. Zhou, Friction and wear behavior of three dimensional braided carbon fiber/epoxy composites under lubricated sliding conditions, Journal of Materials Science 40 (2005) 4475–4481.

[7] K. Efimenko, J.A. Crowe, E. Manias, D.W. Schwark, D.A. Fischer, J. Genzer, Rapid formation of soft hydrophilic silicone elastomer surfaces, Polymer 46 (2005) 9329–9341.

[8] N.W. Khun, E. Liu, G.C. Yang, W.G. Ma, S.P. Jiang, Structure and corrosion behavior of platinum/ruthenium/nitrogen doped diamond-like carbon thin films, Journal of Applied Physics 106 (2009) 013506.

[9] A.W. Neumann, Contact angles and their temperature dependence: thermodynamic status, measurement, interpretation and application, Advances in Colloid and Interface Science 4 (1974) 105–191.

[10] J.S. Chen, S.P. Lau, Z. Sun, G.Y. Chen, Y.J. Li, B.K. Tay, J.W. Chai, Metal-containing amorphous carbon films for hydrophobic application, Thin Solid Films 398 (399) (2001) 110–115.

[11] P. Gabriel, A.G. Thomas, J.J.C. Busfield, Influence of interface geometry on rubber friction, Wear 268 (2010) 747–750.

[12] D.F. Moore, W. Geyer, A review of hysteresis theories for elastomers, Wear 30 (1974) 1–34.

[13] D.F. Moore, W. Geyer, A review of adhesion theories for elastomers, Wear 22 (1972) 113–141.

[14] A.R. Savkoor, Mechanics of sliding friction of elastomers, Wear 113 (1986) 37–60.

[15] C.M. Mate, Tribology on the Small Scale: A Bottom up Approach To Friction, Lubrication and Wear, Oxford University Press, USA, 2008, p. 135.

[16] H. Ronkainen., A. Laukkanen, K. Holmberg, Friction in a coated surface deformed by a sliding sphere, Wear 263 (2007) 1315–1323.

[17] H.W. Kummer, Unified theory of rubber tire friction, Engineering Research Bulletin B-94, Pennsylvania State University, July 1996, p. 89.

[18] T. Hisakado, Effect of surface roughness on contact between solid surfaces, Wear 28 (1974) 217–234.

[19] P.L. Menezes, S.V. Kishore, Kailas, Influence of surface texture and roughness parameters on friction and transfer layer formation during sliding of aluminum pin on steel plate, Wear 267 (2009) 1534–1549.

[20] J. Meng, N.H. Loh, B.Y. Tay, G. Fu, S.B. Torr, Tribological behavior of 316L stainless steel fabricated by micropowder injection molding, Wear 268 (2010) 1013–1019.

[21] M. Bhattacharya, A.K. Bhowmick, Analysis of wear characteristics of natural rubber composites, Wear 269 (2010) 152–166.

[22] J.J.C. Busfield, A.G. Thomas, Indentation tests on elastomer blocks, Rubber Chemistry and Technology 72 (1999) 876–893.

[23] S.W. Zhang, State-of-the-art of polymer tribology, Tribology International 31 (1998) 49–60.

[24] K.A. Grosch, The rolling resistance, wear and traction properties of tread compounds, Rubber Chemistry and Technology 69 (1996) 495–568.

[25] H.W. Kummer, Lubricated friction of rubber discussion, Rubber Chemistry and Technology 41 (1968) 895–907.

[26] A.L. Gal, L. Guy, G. Orange, Y. Bomal, M. Kluppel, Modeling of sliding friction for carbon black and silica filled elastomers on road tracks, Wear 264 (2008) 606–615.